RSC Advances

ROYAL SOCIETY OF CHEMISTRY

www.rsc.org/advances

Cadmium Ion Sorption from Aqueous Solutions by Highly Surface Area Ethylenediaminetetraacetic Acid- and Diethylene Triamine Pentaacetic Acid-Treated Carbon Nanotubes

Ahmad Amiri [a, †], Mehdi Shanbedi[b, *], Maryam Savari[c], Chew Bee Teng[b], S.N. Kazi[b, ‡]

[a] Department of Mechanical Engineering, University of Malaya, Kuala Lumpur, Malaysia

[b] Department of Chemical Engineering, Faculty of Engineering, Ferdowsi University of Mashhad, Mashhad, Iran

[c] Computer Science Department, Faculty of Computer Science & InformationTechnology, University of Malaya, Kuala Lumpur, Malaysia

Corresponding authors:

† E-mail addresses: ahm.amiri@gmail.com & ahm.amiri@siswa.um.edu.my (A. Amiri)

* mehdi.shanbedi@stu-mail.um.ac.ir (M. Shanbedi),

‡ salimnewaz@um.edu.my (S.N. Kazi)

Abstract

A novel and rapid microwave-assisted approach along with Friedel–Crafts acylation has been successfully introduced for functionalization of carbon nanotubes (CNT) via aliphatic and aromatic carboxylic acids. This green and efficient route may play an essential role for realizing miscellaneous functionalizations of CNT, which were successfully functionalized via ethylenediaminetetraacetic acid (EDTA) and diethylene triamine pentaacetic acid (DTPA). Qualitative (FT-IR) and quantitative (TGA, Raman, XPS) characterizations have been employed to investigate the degree of functionalization. The N_2 adsorption isotherm shows the significant increases of 270% and 262% in specific surface area in the low partial pressure region after functionalization of CNT with EDTA and DTPA, respectively, which resulted from eliminating the tube ends or caps. By looking at the potential of EDTA and DTPA for sequestering metal ions, EDTA- & DTPA-treated CNT were used to evaluate the aqueous cadmium (II) adsorption efficiency. Then, the effects of solution temperature, pH and contact time on the adsorption of Cd^{2+} ions onto the treated samples and pristine CNT were investigated. The adsorption performance of Cd^{2+} ions by functionalized samples was illustrated a dramatic growth as compared with the pristine sample, which was effectively pH dependent. The pseudo second-order model precisely captured the kinetic analyses of adsorption. This study suggested that the functionalization method not only enhanced the effective surface area including active

adsorption sites on CNT structure, but also decreased the functionalization time and cost significantly and proposed a promising material for capacitive deionization.

Keywords. Cadmium, Ion Sorption, Carbon Nanotubes, Microwave, EDTA, Functionalization

1. Introduction

Eliminating heavy metals such as lead, cadmium and arsenic from industrial wastewater is a vital environmental parameter[1-3]. It is obvious that most of the heavy metals are non-degradable and they aggregate in different parts of animals and plants, therefore they should be eliminated from industrial wastewater. Cadmium (II) ions as a heavy metal ion is one of the major contaminants of groundwater and surface water, which the metal plating industry play a key role in its production[4, 5]. They aggregate easily in the environment elements such as food chain due to the lack of biodegradability and different diseases such as osteoporosis and anaemia are caused by this heavy metal ion[4, 6-8]. Due to their desirable electrical, mechanical, thermal and chemical properties[9-13], carbon nanotubes (CNT) are promising material with numerous applications[14] such as hydrogen storage[15, 16], catalyst supports[17, 18], chemical sensors[19, 20] etc. As an especial applications, CNT demonstrated an excellent potential for the removal of different heavy metals and many kinds of pollutants from water. CNTs have a large surface area, small hollow, layered structures and a special potential to establish π-π electrostatic interactions[21, 22].

By looking at abovementioned characteristics, CNTs have also illustrated superb adsorption efficiencies and outstanding adsorption capabilities for various organic pollutants and heavy metals, especially in capacitive deionization[23-27].

Unfortunately, a strong intertube van der Waals interaction between the tubes presents weak dispersivity in different solvents, which have been limited the applications of CNT[28]. To improve the interactivity of CNT, chemical functionalization has been suggested as a common technique. The covalent and noncovalent functionalizations were proposed as two efficient approaches for improving the sorption capacity of CNT[29, 30]. Adding carboxylic groups to the surface of CNT under oxidizing conditions with different acids such as HNO_3, H_2SO_4, $KMnO_4$, H_2O_2, and KOH has been reported previously as the efficient routes to enhance the adsorption capabilities of CNT[25-27, 29, 30]. Researchers introduced different functional groups such as COOH, OH, and amines in order to increase the potential of CNT for metal ion sorption[21].

Among the various functional groups attached to the CNT, amino groups together with oxygen groups could serve as electrostatic interaction sites for transition metal sorption[31, 32]. G.D. Vukovi´c et al.[21] reported that the adsorption properties of pristine CNT significantly enhanced by oxidation, as well as by amino-functionalization.

An aminopolycarboxylic acid (complexone) can be selected as a very good candidate due to it is a compound including one or more nitrogen atoms linked through carbon atoms to two or more carboxyl groups. It is obvious that aminopolycarboxylates can form strong complexes with various metal ions. This special potential makes aminopolycarboxylic acids very eligible functional groups for decorating on the surface of CNT to increase metal ion sorption[33].

Between aminopolycarboxylic acids, ethylenediaminetetraacetic acid (EDTA) and diethylene triamine pentaacetic acid (DTPA) are more favorite molecules in sequestering metal ions, because of its ability to sequester different metal ions such as Mn(II), Cu(II), Fe(III), Pb (II) and Co(III) . In order to employ the EDTA functionality, some reflux steps methods such as mixing and sonication can be applied which are commonly time-consuming and comprising multiple steps[34].

Nowadays, the microwave radiation is introduced as a green, rapid and effective approach for functionalization of CNT[35]. It has also confirmed to result in lower structural defects on surface of CNT compared with the common methods[36].

In this study, CNT were first functionalized with EDTA as well as DTPA under microwave radiation in a fast procedure. The pristine, EDTA- and DTPA-treated CNT were then subjected to the chemical and morphological studies. In addition, the possibility of the employed EDTA-and DTPA-treated CNT as a sorbent for the removal of Cd^{2+} ions from aqueous solutions was investigated. Also, the effect of experimental conditions such as reaction time, pH value and temperature on the adsorption behavior was studied.

2. Materials and methods

2.1. Materials

The pristine multi-walled carbon nanotubes prepared by chemical vapor deposition with diameter < 30 nm, length of 5–15 μm and purity > 95% were obtained from Shenzhen Nano-Tech Port Co. Ethylenediaminetetraacetic acid (EDTA), diethylene triamine pentaacetic acid (DTPA), tetrahydrofuran (THF), Methanesulfonic acid ($MeSO_3H$), chloroform and methanol, all with analytical grade, were purchased from Sigma-Aldrich. A stock solution

containing 1000 µg/mL of Cd^{2+} was prepared by dissolving pure-grade cadmium nitrate tetrahydrate ($Cd(NO_3)_2.4H_2O$) and diluted, which was more diluted with deionized water to the required Cd^{2+} concentrations for the sorption measurements.

2.2. Functionalization of CNT

Figure 1a illustrates the schematic diagram of functionalization procedure of CNT with EDTA and DTPA. Recently, the mechanism of Friedel–Crafts acylation of aromatic compounds in the presence of graphite with Methanesulfonic acid ($MeSO_3H$) was described by Hosseini Sarvari and Sharghi [37]. This mechanism with considerable modification was employed for functionalization of CNT with EDTA and DTPA. Interestingly, Hosseini Sarvari and Sharghi [37] reported that their method is simple and highly efficient.

Regarding EDTA-treated CNT, pristine CNT (0.1 gr) and EDTA (1 gr) were mixed and ground for 3 minutes in an agate mortar in a typical experiment. This mixture was then poured into a vessel filled with 20 ml $MeSO_3H$ and sonicated with a probe sonicator (frequency of 20 kHz) for 45 min at 80 °C to get a homogeneous suspension. The reaction mixture was held at 80 °C over above-mentioned period of time and then transferred into an industrial microwave (Milestone MicroSYNTH programmable microwave system) to complete the reaction. The resulting CNT suspension was heated under microwave radiation up to 150 ºC for 15 min with output power of 700 W. The reaction mixture was subsequently cooled, centrifuged with water, ethanol and THF. The obtained black solid washed several times by placing on a Whatman membrane. The obtained product was washed with methanol, chloroform and water to eliminate any unreacted EDTA. Next, the filtration cake was dried for 48 h at 45 ºC. A similar method was employed for the CNT functionalization with DTPA.

2.3. Characterization

The pristine CNT as well as EDTA- and DTPA- treated CNT were characterized by a Fourier transform infrared spectroscopy, FTIR, (Nicolet 470 FTIR), Raman spectroscopy (Renishaw confocal spectrometer at 514 nm), thermo gravimetric analysis, TGA, (Perkin Elmer TGA-7) and X-ray photoelectron spectroscopy (XPS) measurements were performed using MULTILAB 2000 Base system with X-ray with Twin Anode Mg/Al (300/400 W) as X-ray Source. Nitrogen adsorption isotherms at 77 K were measured using a volumetric gas adsorption apparatus (BEL Japan, Belsorp-max). The FTIR spectra of samples were analyzed in the range of 400–4000 cm^{-1} via the KBr pressed disc.

The weight loss was performed in TGA analyzer from 20 to 650 ºC at a heating rate of 10 ◦C min^{-1} in air. Sonication procedure has been done with a probe sonicator, which is comprised of the probe's tips made from titanium. The generator of sonicator provides high voltage pulses of energy at a frequency of 20 kHz.

2.4. Adsorption experiments

The adsorption experiments were performed using a closed 200 ml bottle, containing 1 mg of pristine CNT or treated samples and 10 mL of Cd^{2+} solution (5 $mg.L^{-1}$)[21]. In order to operate at definite temperatures and times, all samples were first placed in an ultrasonic bath. Also, the influence of pH on Cd^{2+} adsorption was investigated between 2.0 and 11.0 using 0.01 and 0.1 $mol.L^{-1}$ NaOH and 0.01 and 0.1 $mol.L^{-1}$ HNO_3 at 25 ºC. The CNT were sonicated with Cd^{2+} solutions for 45 min at 25 ºC and then filtered through a PTFE membrane. The adsorption experiments were carried out at 25, 30 and 40 ºC. In addition, the influence of contact time on Cd^{2+} adsorption was investigated in the range of 5–100 min. As a subsequent analysis, the amount of Cd^{2+} concentrations were measured with the Agilent 7500 ICP-MS. In order to increase the validity of results, all the experiments were done in triplicate and the mean values were announced. Interestingly, the maximum experimental error was less than 3%.

3. Results and discussion

3.1. Functionality analysis

3.1.1. Fourier transform infrared spectroscopy

The FTIR spectra of the pristine CNT and EDTA- and DTPA-treated CNT were illustrated in Figure 1b. As could be seen, the EDTA- and DTPA-treated CNT exhibited apparent cues of different functional groups in contrast to the pristine CNT. A list of peaks and their interpretations were shown in Table 1. The spectrum of EDTA-treated CNT demonstrated peaks at the ranges 3100-3200 cm^{-1} and 3350-3500 cm^{-1}, which could be attributed to the N−H and O−H stretching vibrations. Also, both treated samples spectra illustrated two peaks at the range of 2850-2930 cm^{-1}, which could verify the presence of the C−H stretching vibration. A broad peak at 1673 cm^{-1} was related to the C=O stretching vibrations. Also, another peak at around 1401 cm^{-1} was attributable to the COO^- stretching vibration. The peaks at 1489 cm^{-1} and 1313 cm^{-1} were in agreement with bending vibration of N−H and CH_2 groups. The peaks centered around 1278 cm^{-1} and 1212 cm^{-1} were associated with the C−N and C−O stretching vibrations, respectively[28].

In addition, FTIR spectra showed the strong transmittance peaks around 1673 cm^{-1} because there were plenty of carboxylic groups on CNT surface when EDTA was decorated on the surface of CNT[38].

3.1.2. Thermogravimetric analysis.

The results of thermogravimetric analysis (TGA) of pristine CNT and EDTA- and DTPA-treated CNT were shown in Figure 1c. Although the TGA curve of the pristine CNT illustrated no considerable weight loss up to 500 ºC, the treated samples presented special weight loss in the temperature range of 100–300 ºC.

The first weight loss presented in the temperature range of 100–300 ºC could be attributed to the functionalities of EDTA and DTPA as an unstable organic part on the structure of CNT. The second part of weight loss in the temperature range of 500–600 ºC showed the decomposing of the main graphitic structures in air. Also, TGA and FTIR results showed a good agreement in terms of CNT functionalization with EDTA and DTPA[10, 28].

3.1.3. Raman Spectroscopy

Raman spectroscopy can be employed to characterize different functional groups as well as can play a key role in estimating the degree of covalent functionalization.

The Raman spectra of the pristine and EDTA- and DTPA-treated CNT were shown in Figure 1d, which illustrated the D and G bands at 1346 and 1576 cm^{-1}, respectively. The G band at 1576 cm^{-1} was related to the movement in opposed direction of two nigh carbon atoms in the graphitic sheets. This pattern obviously shows the presence of graphitic carbon in CNT. On the other hand, the D band at 1346 cm^{-1} was attributed to the amorphous/disordered carbon, which resulted by the addition of functional groups to the main structure. Commonly, the intensity ratios of D and G bands (I_D/I_G) are considered as the ratio of amorphous carbon (sp^3) to graphitic carbon (sp^2)[39]. As could be seen in Figure 1d, I_D/I_G values of EDTA- and DTPA-treated CNT were more than pristine CNT, which indirectly proposed successful functionalization of the pristine CNT and implying more structure defects. In the field of functionalization, the higher ratio of peak intensities (I_D/I_G) demonstrates the higher extent of covalent functionalization and greater extent of C=C rupture. According to the results, the sequence of the intensity ratio was as follow:

EDTA-treated CNT = DTPA-treated CNT > Pristine CNT.

Despite the intensity ratio between the functionalized CNT with EDTA and DTPA was negligible, it can play an essential role for industrial production. TGA and Raman results were confirmed the functionalization of CNT with EDTA and DTPA. In addition, Raman results established an equal tendency for EDTA and DTPA to react with CNT.

3.1.4. X-ray photoelectron spectroscopy (XPS)

The nature of pristine CNT, EDTA- and DTPA-treated CNT are studied by X-ray photoelectron spectroscopy (XPS), which are illustrated in Figure 2 and Table 2. The XPS wide spectra of pristine CNT, EDTA and DTPA-treated samples are shown in Figure 2a, b and c, respectively. It can be seen that C 1 s and O 1 s peaks appear at 284.5 eV and 531.8 eV [40, 41]. Based on results, while pristine CNT presents a weak peak of oxygen, the intensity of O 1 s peak growths considerably in EDTA- and DTPA-treated CNT samples. It is obvious that EDTA and/or DTPA functionalities may explain the higher content of oxygen in CNT after functionalization. Also, as shown in Figure 2b and c, the characteristic peaks of the N element were observed.

To investigate the nature of functional groups, further study has been carried out by the high-resolution C 1 s scans. Figure 2d and 2e present the deconvoluted C1s spectra of EDTA- and DTPA-treated CNT, respectively. Both treated samples (Figure 2b and e) illustrate a peak at the binding energy at 284.6 eV, which was assigned to the carbon skeleton (C–C/C=C). Also, the binding energies at 286.1 and 287.3 eV were attributed to the C–O and C=O of the EDTA and/or DTPA functionalities. Consist with XPS results, the signal at about 285.0 eV was assigned to the C–N (from amide bond in EDTA/DTPA). These results further indicated that the CNT was successfully functionalized with EDTA and DTPA[42, 43].

3.1.5. BET surface area and PH analysis

The physical properties of the pristine CNT, EDTA- and DTPA-treated CNT were shown in Table 3 and Figure 3. It is evident that the surface area of EDTA-treated CNT and DTPA-treated CNT were significantly higher than those of the pristine CNT.

Again, the surface area of EDTA-treated CNT and DTPA-treated CNT increased significantly after functionalization (Figure 3). Commonly, eliminating the tube ends or caps has been performed via different chemical approaches and the effective surface area has been reported to enhance 50–380% after opening the tubes[44]. Also, the chemical

modification of CNT with oxidant acids and other functional groups enhances the external diameters of the carbon nanostructures[45, 46]. Accordingly, based on the present results, the surface area were 104, 386 and 377 $m^2.g^{-1}$ in pristine CNT, EDTA- and DTPA-treated CNT, respectively. Due to the short microwave heating and reaction time, it is obvious that the external diameters could not be increased[45], thus the main reason for these enhancement after functionalization is attributed to the opening the tube caps under severe condition of microwave. According to the previous experimental results[45, 47-49], CNT functionalization under microwave irradiation can also produce some structural defects in addition to eliminating tubes ends. The higher specific surface area can provide more suitable condition for cadmium (II) adsorption. The N_2 adsorption isotherm (Figure 3) shows a significant increase in specific surface area in the low partial pressure region after functionalization of CNT with both EDTA and DTPA.

3.1.6. Scanning and transmission electron microscopy

Figure 4 panels (a) and (b) present SEM images of the EDTA- and DTPA-treated CNT, respectively. It can be seen that both samples retained the cylindrical cross-section of tubes. As a more evidence with higher quality, TEM images of the EDTA- and DTPA-treated CNT are shown in Figure 4c and 4d, respectively. In the both images, one can see multi-walled CNT with relatively smooth and intact walls and low wall-defected CNT. On the other hand, cut and open ends of CNT are obvious after functionalization by EDTA and DTPA, which could be the result from the severe functionalization condition under microwave irradiation.

3.2. Adsorption studies

The Cd^{2+} adsorption behavior of pristine CNT, EDTA-treated CNT and DTPA-treated CNT was studied at a pH range of 2.0 to 11.0 (Figure 5). Adsorption of Cd^{2+} on EDTA-treated CNT and DTPA-treated CNT was significantly dependent on the pH of solution. It is obvious that there is a direct connection between the pH value and the surface charge of treated CNT. Also, the degree of ionization, the morphology and physical properties of carbon nanostructure can be influenced by the pH of the solution[21]. Commonly, cadmium molecule in deionized water be able to present in the forms of Cd^{2+}, $Cd(OH)^+$, $Cd(OH)_2$, etc.[21, 50] .Interestingly, a certain amount of cadmium molecule in water at pH below 9 is Cd^{2+} in the form of complex $[Cd(H_2O)_6]^{2+}$ [51].

As could be seen, EDTA-treated CNT and DTPA-treated CNT showed significantly higher adsorption capacities than pristine CNT. In addition, although the difference in adsorption capacities of treated samples was

negligible, it could be noticed that DTPA-treated CNT illustrated the best adsorption capacities at different pH values (Figure 5). On the other hand, Cd^{2+} adsorption on the pristine CNT resulted in a slight pH dependence. There was a considerable growth in Cd^{2+} adsorption at the pH range of 4 to 6 for treated CNT with EDTA and DTPA. A pH value more than 6 is capable for the ionization of the acidic functional groups in EDTA and DTPA, which play a vital role in adsorption of Cd^{2+} ions. Vukovi´c et al. concluded that the negative charges created in the CNT surface at pH lower than pH_{PZC} increased the cation-exchange capacity of oxidized CNT[52]. Due to the poor dissociation of the carboxylic groups on the surface of CNT and competition between H^+ and Cd^{2+} ions for the same adsorption site, the performance of Cd^{2+} adsorption at the pH range of 2 to 4 was insignificant[30]. EDTA and DTPA are mostly applied for sequestering metal ions and generally bind to metal cations through its amines and carboxylates groups. According to abovementioned properties, the performance of Cd^{2+} adsorption of EDTA-treated CNT and DTPA-treated CNT at the pH range of 2 to 4 were higher than oxidized CNT with different acids and functionalized CNT with ethylenediamine[21, 45].

The adsorption capacity of treated samples has undergone a significant drop at the pH values higher than 9.0, which was in agreement with the drop in the Cd^{2+} concentration. Furthermore, sedimentation of $Cd(OH)_2$ at the pH range more than 10 occupied most of adsorption sites in the presence of both EDTA- and DTPA-treated CNT, which resulted in lower Cd^{2+} sorption as the pH enhanced [21].

Figure 6 illustrated the kinetic analysis of the adsorption of Cd^{2+} onto the pristine CNT, EDTA-and DTPA-treated CNT as a function of contact time. The Cd^{2+} adsorption onto pristine CNT and treated samples has been enhanced dramatically over 0.5 h of contact time, and subsequently slowed. Unsurprisingly, abundant vacant sites on CNT surface were available for Cd^{2+} adsorption over the initial stage. As the time went by, the repulsive forces between the Cd^{2+} molecules on the CNT surface and the bulk phase increased, consequently the remaining vacant sites could not be simply occupied[45].

As could be seen, thirty minutes were sufficient to achieve the adsorption equilibrium. A majority of previous studies confirmed that the pseudo second-order models can be selected as the best model for CNT samples[21, 30, 53]. So, the pseudo second-order rate equation was employed in this study. The kinetic rate equations could be used as follows:

$$\frac{t}{q_t} = \frac{1}{K{q_e}^2} + \frac{1}{q_e}t \quad (1)$$

where K is the pseudo-second-order rate constant of adsorption (g mg^{-1} min^{-1}), q_e the amount of metal ions adsorbed ($mg.g^{-1}$) at equilibrium, and q_t is the amount of metal ions adsorbed on the surface of the CNT samples at time t ($mg.g^{-1}$). Pseudo second-order model was compared with the experimental data to investigate the validity of mentioned model (Table 4 & Figure 6). According to the regression analysis (R^2), the pseudo second-order rate equation demonstrated an excellent agreement with experimental data. Table 4 presented the kinetic parameters of the pseudo second-order equation for Cd^{2+} adsorption on pristine CNT, EDTA-CNT and DTPA-CNT, which the R^2 values of the second-order model were more than 0.99 for all samples. Moreover, the calculated q_e values with the pseudo second-order model were in agreement with the experimental q_e values.

A plot of t/q_t against t was illustrated in Figure 7. It is obvious that K value is constant, so it could be concluded that Cd^{2+} adsorption to achieve equilibrium onto pristine CNT was faster than those of both functionalized samples. The slower adsorption rates on EDTA-treated CNT and DTPA-treated CNT demonstrates that processes with higher energetic barrier[21, 30] like chemisorption are more operative.

The adsorption of Cd^{2+} on EDTA- and DTPA-treated CNT as the functions of contact time and temperature at 25, 35 and 45 ◦C were shown in Figure 8. As could be seen, as the temperature increased, the Cd^{2+} adsorption performance increased. For example, Cd^{2+} adsorption of DTPA-CNT at 45 ºC improved more than 5% compared with that of DTPA-treated CNT at 25 ◦C at a fixed time of 30 min.

4. Conclusion

This study first introduced a new, efficient, green and fast method for functionalization via EDTA and DTPA. EDTA and DTPA were successfully decorated on the surface of CNT via Friedel–Crafts acylation in a microwave-assisted technique, which resulted in a high degree of functionalization. Based on the qualitative and quantitative results, functionalization of CNT with above-mentioned groups was confirmed. Then, the equilibrium adsorption of Cd^{2+} onto pristine and functionalized CNT with EDTA and DTPA were investigated at different pH values and temperatures. The adsorption capacity of aqueous cadmium (II) onto functionalized CNT enhanced with the temperature. The negatively charged surfaces of functionalized CNT electrostatically favored the adsorption of Cd^{2+} in DTPA-treated CNT more than EDTA- treated CNT. The kinetic analyses of adsorption were carried out using pseudo second-order models and the regression results confirmed that a pseudo second-order model well fitted the

adsorption kinetics. These results verify the capacity of EDTA- and DTPA-treated CNT in manufacture of filtration membranes for the elimination of the heavy metals from industrial waters.

Acknowledgements

The authors gratefully acknowledge Bright Sparks Unit of the University of Malaya, UMRG Grant RP012B-13AET and High Impact Research Grant UM.C/625/1/HIR/MOHE/ENG/45, Faculty of Engineering, University of Malaya, Malaysia for support to conduct this research work.

References

1. Z. Ali, R. Ahmad and A. Khan, *RSC Advances*, 2014, **4**, 50056-50063.
2. M. A. Melo Jr, C. T. G. V. M. T. Pires and C. Airoldi, *RSC Advances*, 2014, **4**, 41028-41038.
3. Q. Zhang, J. Teng, Z. Zhang, G. Nie, H. Zhao, Q. Peng and T. Jiao, *RSC Advances*, 2015, **5**, 55445-55452.
4. A. Corami, S. Mignardi and V. Ferrini, *Journal of Colloid and Interface Science*, 2008, **317**, 402-408.
5. C.-H. Wu, *Journal of colloid and interface science*, 2007, **311**, 338-346.
6. S. Mandjiny, K. Matis, A. Zouboulis, M. Fedoroff, J. Jeanjean, J. Rouchaud, N. Toulhoat, V. Potocek, C. Loos-Neskovic and P. Maireles-Torres, *Journal of materials science*, 1998, **33**, 5433-5439.
7. M. Kazemipour, M. Ansari, S. Tajrobehkar, M. Majdzadeh and H. R. Kermani, *Journal of Hazardous Materials*, 2008, **150**, 322-327.
8. D. Marchat, D. Bernache-Assollant and E. Champion, *Journal of hazardous materials*, 2007, **139**, 453-460.
9. M. F. L. De Volder, S. H. Tawfick, R. H. Baughman and A. J. Hart, *Science*, 2013, **339**, 535-539.
10. A. Amiri, R. Sadri, G. Ahmadi, B. Chew, S. Kazi, M. Shanbedi and M. S. Alehashem, *RSC Advances*, 2015, **5**, 35425-35434.
11. A. Amiri, M. Shanbedi, H. Amiri, S. Z. Heris, S. Kazi, B. Chew and H. Eshghi, *Applied Thermal Engineering*, 2014, **71**, 450-459.
12. H. Z. Zardini, M. Davarpanah, M. Shanbedi, A. Amiri, M. Maghrebi and L. Ebrahimi, *Journal of Biomedical Materials Research Part A*, 2014, **102**, 1774-1781.
13. H. Zare-Zardini, A. Amiri, M. Shanbedi, A. Taheri-Kafrani, S. Kazi, B. T. Chew and A. Razmjou, *Journal of Biomedical Materials Research Part A*, 2015.
14. Q. Zhang, J.-Q. Huang, W.-Z. Qian, Y.-Y. Zhang and F. Wei, *Small*, 2013, **9**, 1237-1265.
15. W. Liu, Y. H. Zhao, Y. Li, Q. Jiang and E. J. Lavernia, *The Journal of Physical Chemistry C*, 2009, **113**, 2028-2033.
16. B. Chakraborty, P. Modak and S. Banerjee, *The Journal of Physical Chemistry C*, 2012, **116**, 22502-22508.
17. M. Moghadam, S. Tangestaninejad, V. Mirkhani, I. Mohammedpoor-Baltork, A. Mirjafari and N. S. Mirbagheri, *J. Mol. Catal. A: Chem.*, 2010, **329**, 44-49.
18. N. Nagaraju, A. Fonseca, Z. Konya and J. B. Nagy, *J. Mol. Catal. A: Chem.*, 2002, **181**, 57-62.
19. G. P. Evans, D. J. Buckley, N. T. Skipper and I. P. Parkin, *RSC Advances*, 2014, **4**, 51395-51403.
20. M. K. Bayazit, L. O. Palsson and K. S. Coleman, *RSC Advances*, 2015, **5**, 36865-36873.

21. G. D. Vuković, A. D. Marinković, M. Čolić, M. Đ. Ristić, R. Aleksić, A. A. Perić-Grujić and P. S. Uskoković, *Chemical Engineering Journal*, 2010, **157**, 238-248.
22. F. Su, C. Lu and S. Hu, *Colloids and Surfaces A: Physicochemical and Engineering Aspects*, 2010, **353**, 83-91.
23. A. Gadhave and J.Waghmare, *International Journal of Chemical Sciences and Applications*, 2014, **5**, 56-67
24. O. Moradi, K. Zare and M. Yari, *Int.J.Nano.Dim*, 2011, **1**, 203-220.
25. G. P. Rao, C. Lu and F. Su, *Separation and Purification Technology*, 2007, **58**, 224-231.
26. K. Yang, W. Wu, Q. Jing and L. Zhu, *Environmental science & technology*, 2008, **42**, 7931-7936.
27. C. Lu and H. Chiu, *Chemical Engineering Journal*, 2008, **139**, 462-468.
28. A. Amiri, M. Shanbedi, H. Eshghi, S. Z. Heris and M. Baniadam, *The Journal of Physical Chemistry C*, 2012, **116**, 3369-3375.
29. Z. Gao, T. J. Bandosz, Z. Zhao, M. Han and J. Qiu, *Journal of Hazardous Materials*, 2009, **167**, 357-365.
30. D. Xu, X. Tan, C. Chen and X. Wang, *Journal of Hazardous Materials*, 2008, **154**, 407-416.
31. S. Deng and Y.-P. Ting, *Water Research*, 2005, **39**, 2167-2177.
32. J. Yu, M. Tong, X. Sun and B. Li, *Journal of hazardous materials*, 2007, **143**, 277-284.
33. G. Anderegg, F. Arnaud-Neu, R. Delgado, J. Felcman and K. Popov, *Pure and applied chemistry*, 2005, **77**, 1445-1495.
34. S. Z. Heris, M. Fallahi, M. Shanbedi and A. Amiri, *Heat and Mass Transfer*, 2015, 1-9.
35. B. Ghiadi, M. Baniadam, M. Maghrebi and A. Amiri, *Russian Journal of Physical Chemistry A*, 2013, **87**, 649-653.
36. E. Vázquez and M. Prato, *ACS Nano*, 2009, **3**, 3819-3824.
37. M. Hosseini Sarvari and H. Sharghi, *Synthesis*, 2004, 2165-2168.
38. C.-r. Tang, G. Tian, Y.-j. Wang, Z.-h. Su, C.-x. Li, B.-g. Lin, H.-w. Huang, X.-y. Yu, X.-f. Li and Y.-f. Long, *Bulletin of the Chemical Society of Ethiopia*, 2009, **23**.
39. M. Shanbedi, S. Z. Heris, A. Amiri and M. Baniadam, *Journal of Dispersion Science and Technology*, 2014, **35**, 1086-1096.
40. S. F. Seyed Shirazi, S. Gharehkhani, H. Yarmand, A. Badarudin, H. S. Cornelis Metselaar and S. N. Kazi, *Materials Letters*, 2015, **152**, 192-195.
41. S. Gharehkhani, S. F. S. Shirazi, S. Pilban-Jahromi, M. Sookhakian, S. Baradaran, H. Yarmand, A. A. Oshkour, S. N. Kazi and W. J. Basirun, *RSC Advances*, 2015.
42. L. Ma, H. Qin, C. Cheng, Y. Xia, C. He, C. Nie, L. Wang and C. Zhao, *Journal of Materials Chemistry B*, 2014, **2**, 363-375.
43. Y. Yu, Y. Sun, C. Cao, S. Yang, H. Liu, P. Li, P. Huang and W. Song, *Journal of Materials Chemistry A*, 2014, **2**, 7706-7710.
44. J. H. Lehman, M. Terrones, E. Mansfield, K. E. Hurst and V. Meunier, *Carbon*, 2011, **49**, 2581-2602.
45. C.-Y. Kuo and H.-Y. Lin, *Desalination*, 2009, **249**, 792-796.
46. Y.-H. Li, S. Wang, Z. Luan, J. Ding, C. Xu and D. Wu, *Carbon*, 2003, **41**, 1057-1062.
47. J. Ruparelia, S. Duttagupta, A. Chatterjee and S. Mukherji, *Desalination*, 2008, **232**, 145-156.
48. M. Monthioux, B. Smith, B. Burteaux, A. Claye, J. Fischer and D. Luzzi, *Carbon*, 2001, **39**, 1251-1272.
49. A. Amiri, M. Maghrebi, M. Baniadam and S. Z. Heris, *Applied Surface Science*, 2011, **257**, 10261-10266.
50. R. Leyva-Ramos, J. Rangel-Mendez, J. Mendoza-Barron, L. Fuentes-Rubio and R. Guerrero-Coronado, *Water Science and Technology*, 1997, **35**, 205-211.

51. K. Ozutsumi, T. Takamuku, S.-i. Ishiguro and H. Ohtaki, *Bulletin of the Chemical Society of Japan*, 1989, **62**, 1875-1879.
52. C. Lu and C. Liu, *Journal of Chemical Technology and Biotechnology*, 2006, **81**, 1932-1940.
53. C.-Y. Kuo, *Journal of hazardous materials*, 2008, **152**, 949-954.

Figure and Table Captions:

Figure 1. (a) Schematic illustration of the functionalization of CNT with EDTA and DTPA, (b) FTIR spectra of pristine CNT, EDTA- and DTPA-treated CNT, (c) TGA curves of pristine CNT, EDTA- and DTPA-treated CNT and (d) Raman spectra of pristine CNT, EDTA- and DTPA-treated CNT.

Figure 2. XPS wide scan of the (a) pristine CNT, (b) EDTA-treated CNT, (c) DTPA-treated CNT and C 1 s core level spectra of the (d) EDTA-treated CNT and (e) DTPA-treated CNT.

Figure 3. Nitrogen adsorption/desorption at 77 K for pristine CNT, EDTA-treated CNT and DTPA-treated CNT.

Figure 4. SEM image of (a) the EDTA-treated CNT, (b) DTPA-treated CNT and TEM image of (c) EDTA-treated CNT and (d) DPTA-treated CNT.

Figure 5. Effect of pH on the adsorption of Cd^{2+} on pristine CNT, EDTA-treated CNT and DTPA-treated CNT [C_0 (Cd^{2+}) = 5 mg L^{-1} and T = 25 ºC].

Figure 6. Effect of time on the sorption of Cd^{2+} by pristine CNT, EDTA-treated CNT and DTPA-treated CNT [C_0 (Cd^{2+}) = 5 mg L^{-1} and T = 25 ºC, m/V=100 mg L^{-1}].

Figure 7. Pseudo-second-order kinetics for the sorption of Cd^{2+} by pristine CNT, EDTA-treated CNT and DTPA-treated CNT [C_0 (Cd^{2+}) = 5 mg L^{-1}, PH=8 and T = 25 ºC, m/V=100 mg L^{-1}].

Figure 8. Adsorption isotherms of Cd^{2+} on the EDTA-treated CNT and DTPA-treated CNT at 25, 35 and 45 ºC.

Table 1. Fourier transform infrared interpretation of the EDTA- and DTPA- treated CNT

Table 2. Peak positions of various groups in C1s spectra of EDTA- and DTPA-treated CNT.

Table 3. Physical properties of pristine CNT, EDTA- and DTPA-treated CNT.

Table 4. Kinetic parameters of the pseudo second-order equation for Cd^{2+} adsorption on pristine CNT, EDTA-treated CNT and DTPA-treated CNT.

Table 1. Fourier transform infrared interpretation of the EDTA- and DTPA- treated CNT

Peak(cm^{-1})	**Interpretation**
3350-3500	O–H stretching vibration
3000-3200	N–H stretching vibration
2850-2930	C–H stretching vibration
1611	–C=O stretching vibration
1443	–NH bending vibration
1385	COO^- Stretching vibration
1288	CH_2 bending vibration
1243	C–N stretching vibration
1210	C–O stretching vibration

Table 2. Peak positions of various groups in C1s spectra of EDTA- and DTPA-treated CNT.

Sample	functional group peak positions (eV)			
	C-C/C=C	C-O	C=O	C-N
EDTA-treated CNT	284.4	286.1	287.3	284.9
DTPA-treated CNT	284.5	286.2	287.3	285

Table 3. Physical properties of pristine CNT, EDTA- and DTPA-treated CNT.

Sorbents	Surface area ($m^2.g^{-1}$)	Pore volume ($cm^3.g^{-1}$)
Pristine CNT	104.12	0.04
EDTA-treated CNT	386.27	0.14
DTPA-treated CNT	377.11	0.14

Table 4. Kinetic parameters of the pseudo second-order equation for Cd^{2+} adsorption on pristine CNT, EDTA-treated CNT and DTPA-treated CNT.

Sample	**$q_{e,\,exp}$ (mg g^{-1})**	**$q_{e,\,cal}$ (mg g^{-1})**	**K (g mg^{-1} min^{-1})**	**R^2**
Pristine CNT	1.59	1.67	0.175	0.994
EDTA-treated CNT	44.34	45.45	0.0285	0.999
DTPA-treated CNT	46.97	47.61	0.0294	0.999

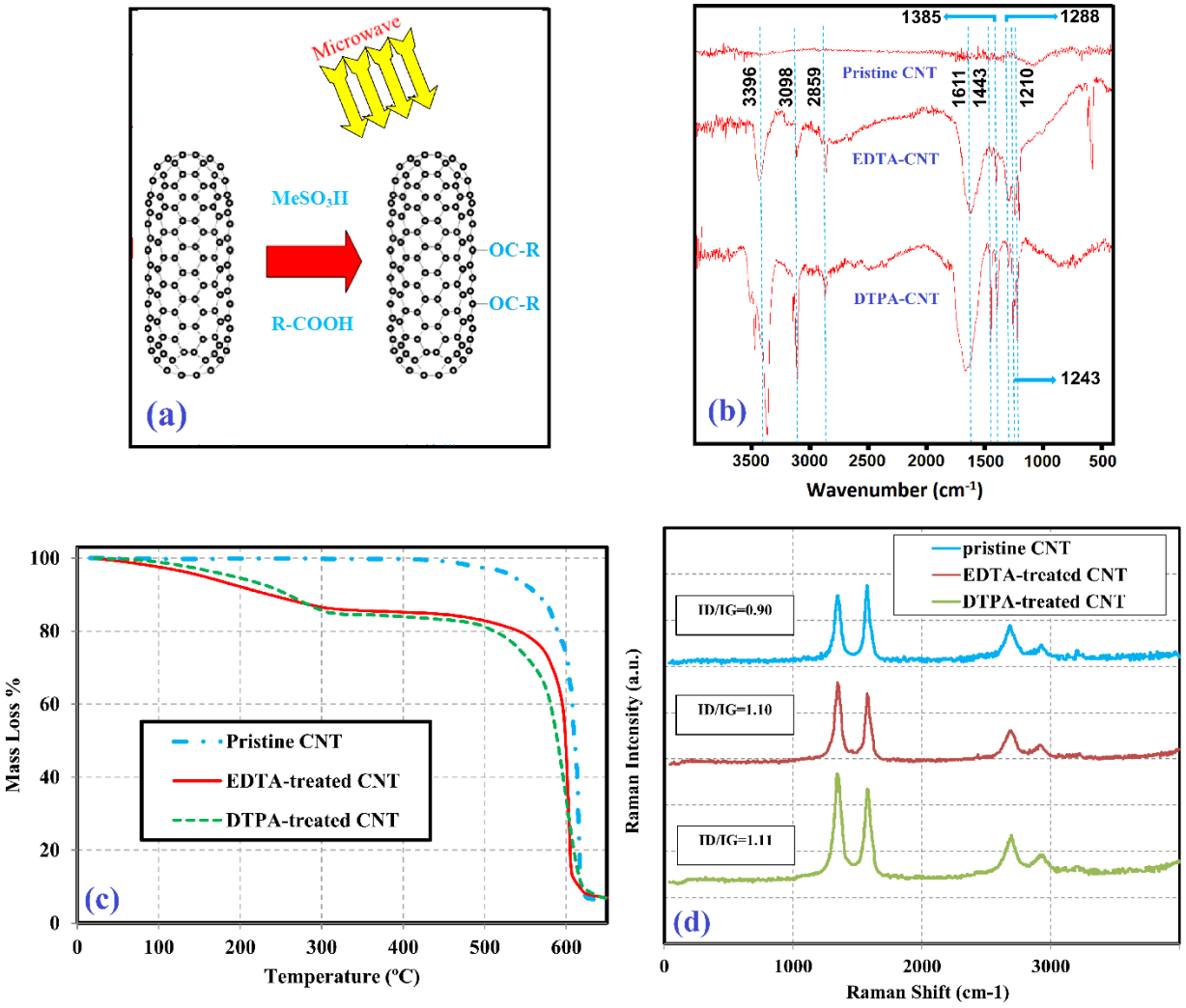

Figure 1

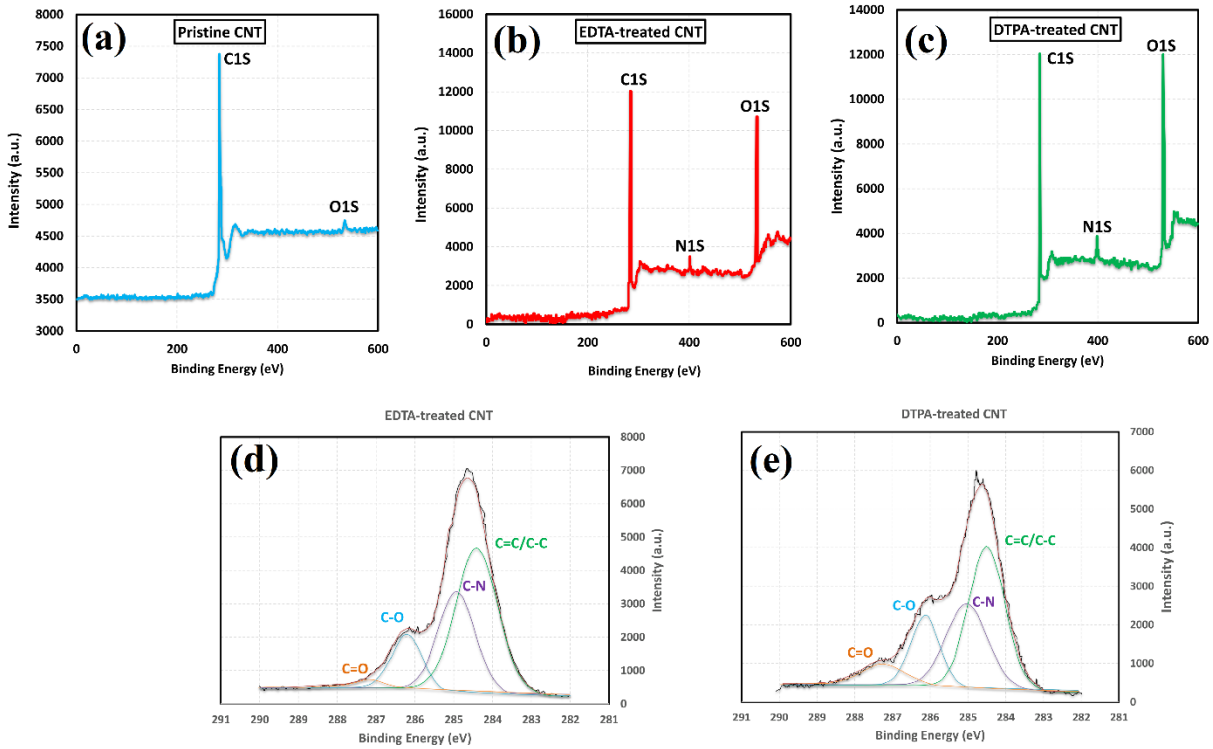

Figure 2

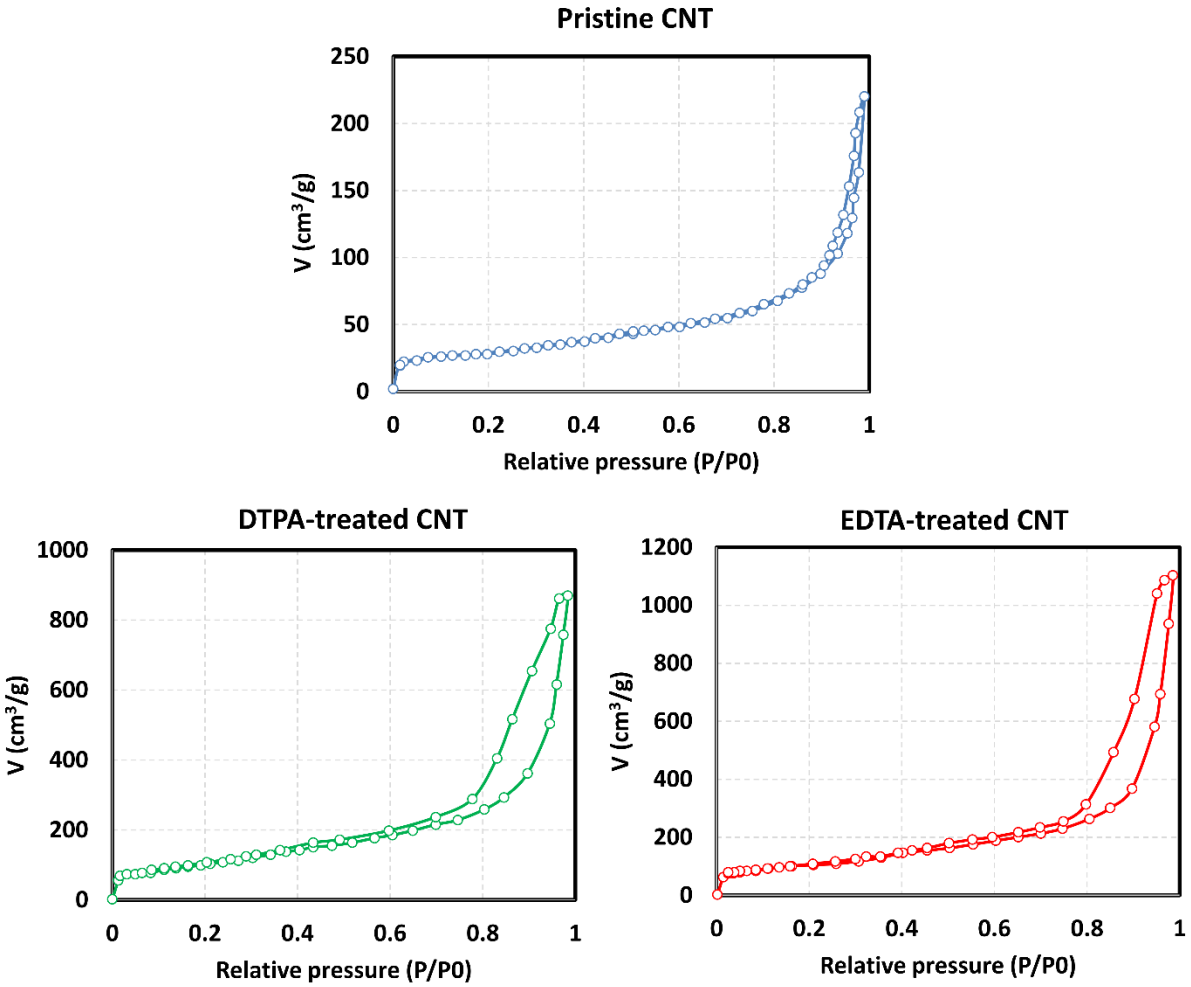

Figure 3

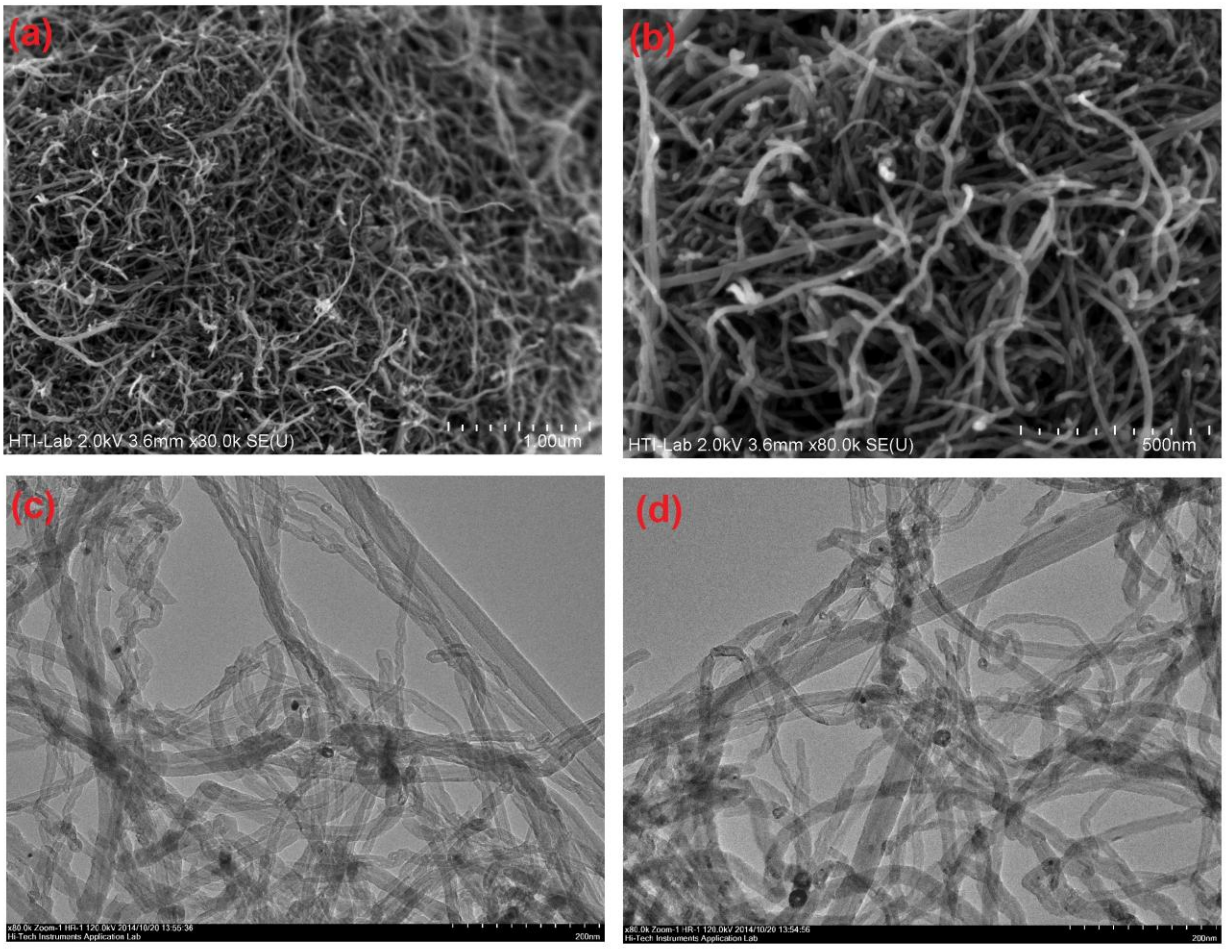

Figure 4

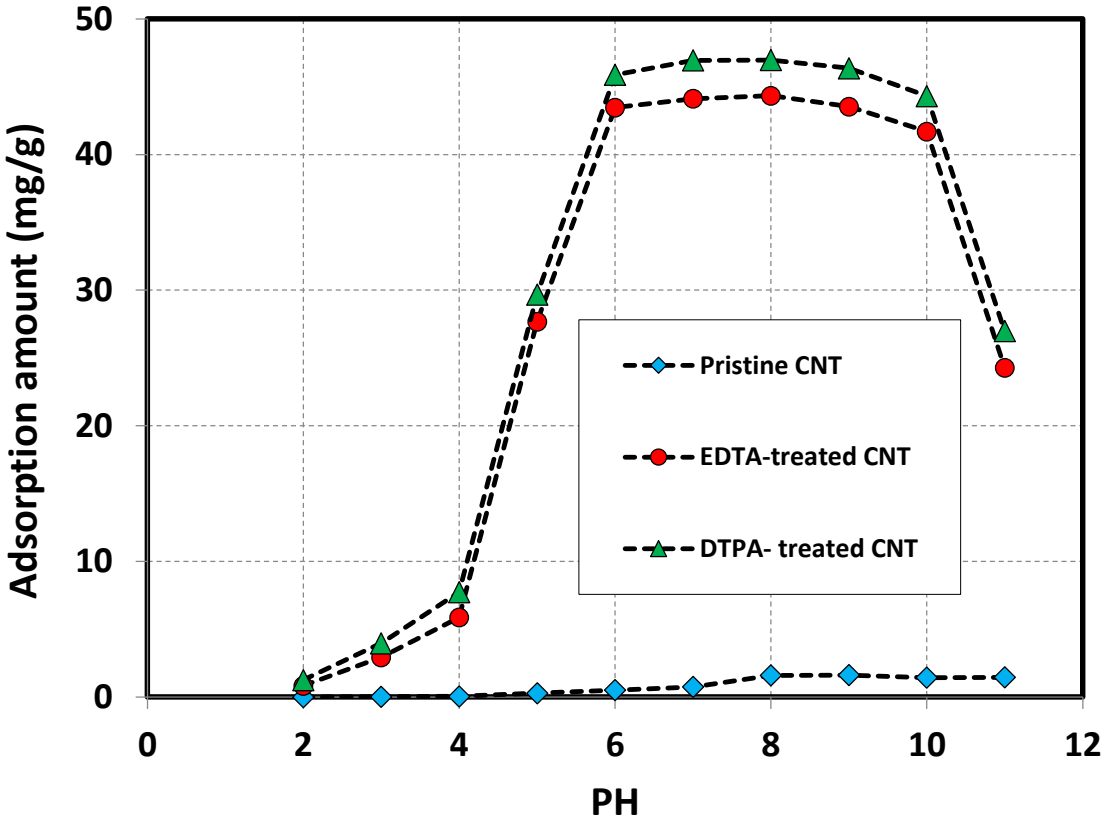

Figure 5

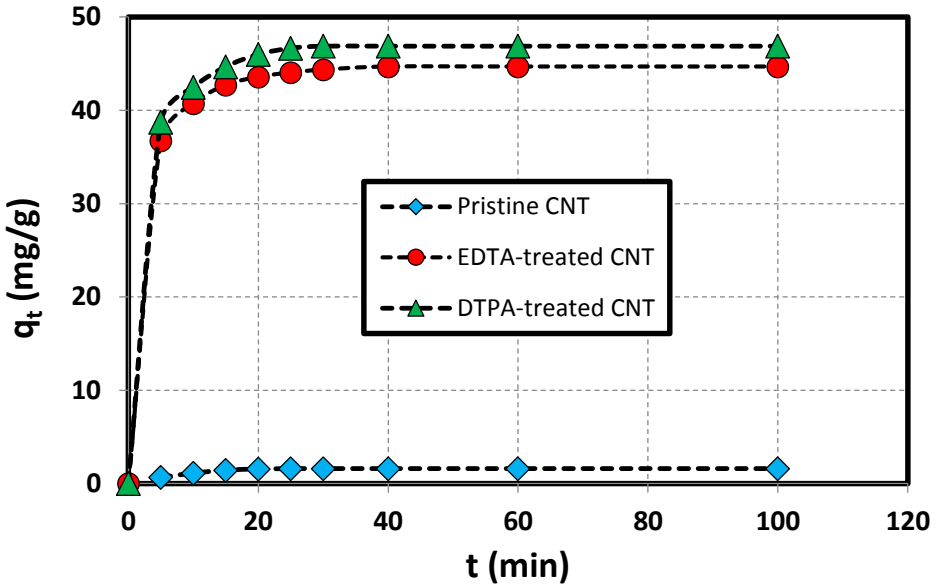

Figure 6

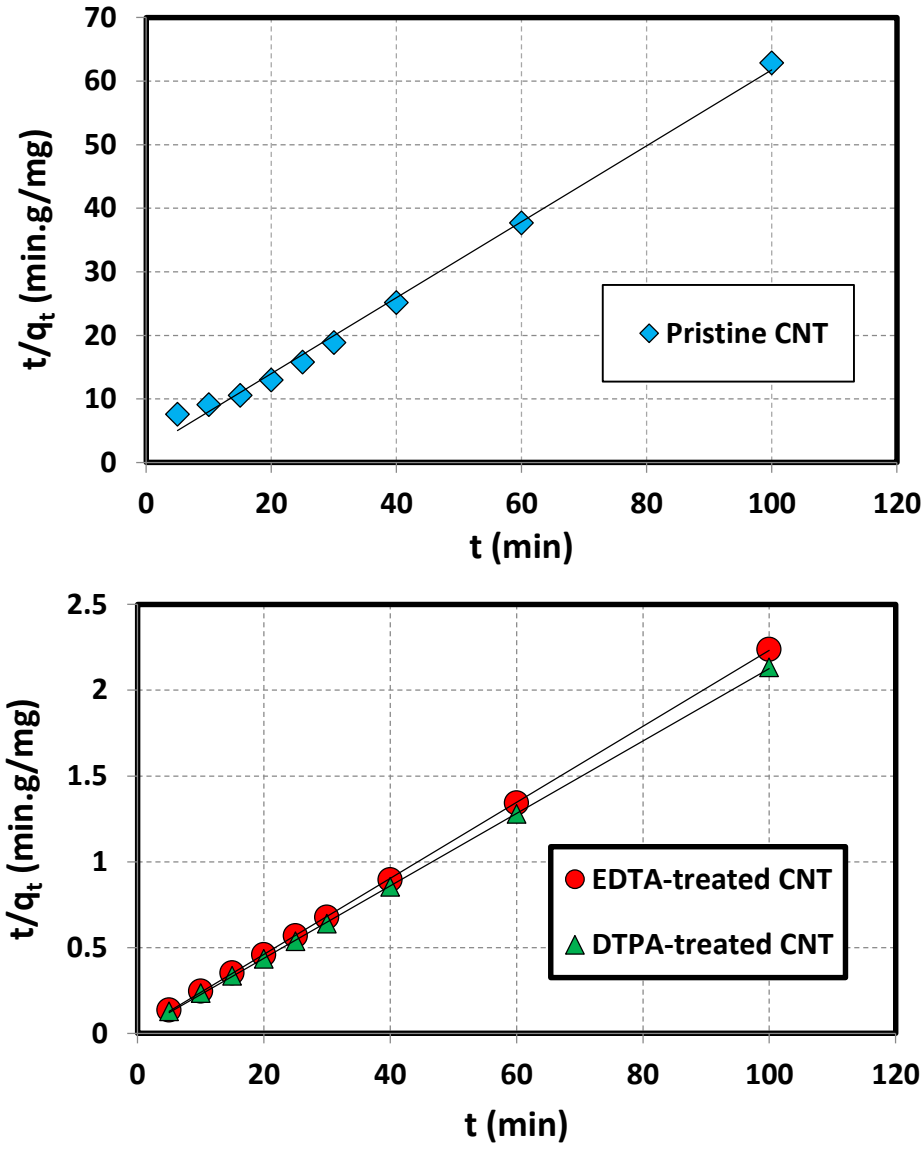

Figure 7

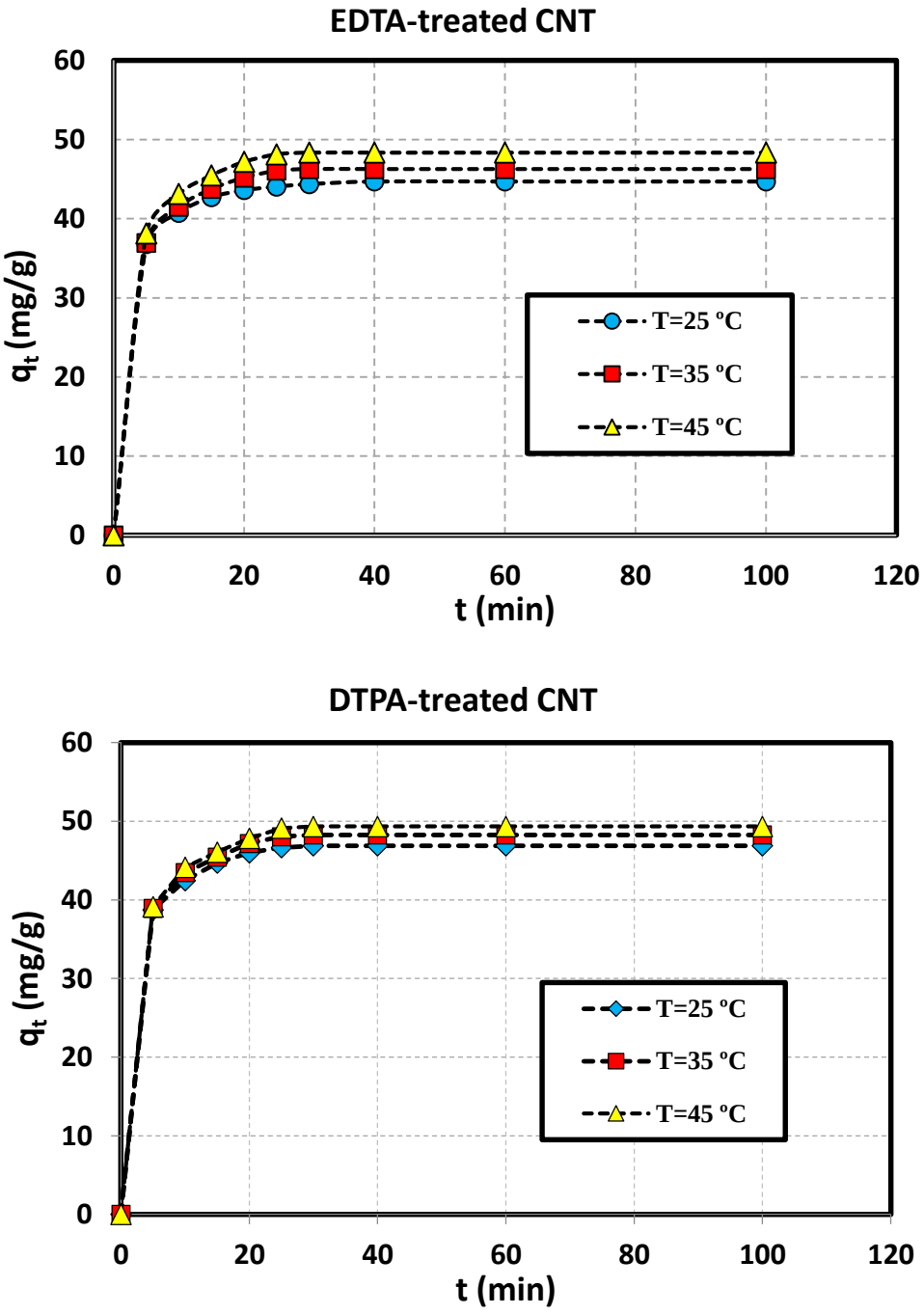

Figure 8